Natural Convection in Below Grade Open Cell Concrete Block Walls

Merle F. McBride, Ph.D., P.E.
Life Member ASHRAE

ABSTRACT

A series of eight calibrated hot box experimental tests were completed to determine the impact of natural convection in below grade open cell concrete block walls. The thermal boundary conditions associated with the exterior soil were included by using a tapered layer of insulation. Once the tests were completed with the open cells they were then filled with sand to eliminate any convection affects and retested. The key challenge was to investigate the 38% over-prediction of the R-value of walls insulated only on the top half by the arc-length method. The results were intended to be used to further develop a simplified analytical model that can estimate the energy savings with various insulation strategies on the interior or exterior at full depth or partial depths. Key findings were that the heat transfer in the hollow cores is extremely complex and driven primarily by natural convection but also includes radiation and conduction through the webs and shell faces of the concrete blocks. Natural convection was identified as the major driving force. The results did not lead to any new modeling procedures or correlations that would improve the arc length model. Future modeling improvements will need to focus on a thermal network that simultaneously accounts for all of the heat transfer mechanisms.

INTRODUCTION

The thermal performance of below grade masonry block walls is complex and influenced by the surrounding soil which makes it a two dimensional heat transfer problem with natural convection and radiation within the block cavities and vertical heat transfer through the concrete webs and face shells. The thermal boundary conditions associated with the exterior soil were experimentally investigated by using a tapered layer of insulation. The four cases of interior insulation tested in a calibrated hot box were: (1) no insulation, (2), R-5 (R-0.9) full wall, (3) R-11 (R-1.9) full wall and (4) R-11 (R-1.9) on just the top half of the wall. Once the four open cell tests were completed the cells were then filled with sand to eliminate convection affects and retested.

The results of these tests were initially analyzed using a one-dimensional steady-state, concentric arc heat-flow path, "series-parallel" (isothermal planes) procedure (Shipp-1983), see Figure 1. The average difference between the measured and predicted wall thermal resistances was 4% with sand filled cavities and 6% with open cavities except when the insulation only covered the top half of the interior surface. For that case the predicted thermal resistance was 38% greater than the measured value.

It was concluded that the simplified model was adequate except for the case when the wall cavities are empty and the wall was insulated only on the top half.

DESCRIPTION OF THE THERMAL TESTS

The thermal performance of below grade masonry block walls was investigated through a series of eight steady-state calibrated hot box (CHB) tests for a variety of constructions in a 9 ft (2.7 m) high by 14 ft (4.3 m) wide test frame, see Figure 2. Heat flux transducers and thermocouples were installed on the interior and exterior surfaces of the masonry block wall to define six thermal nodes. All of the tests used an interior air

Dr. McBride *is a Senior Research Associate at the Owens Corning Center of Science and Technology, Granville, OH.*

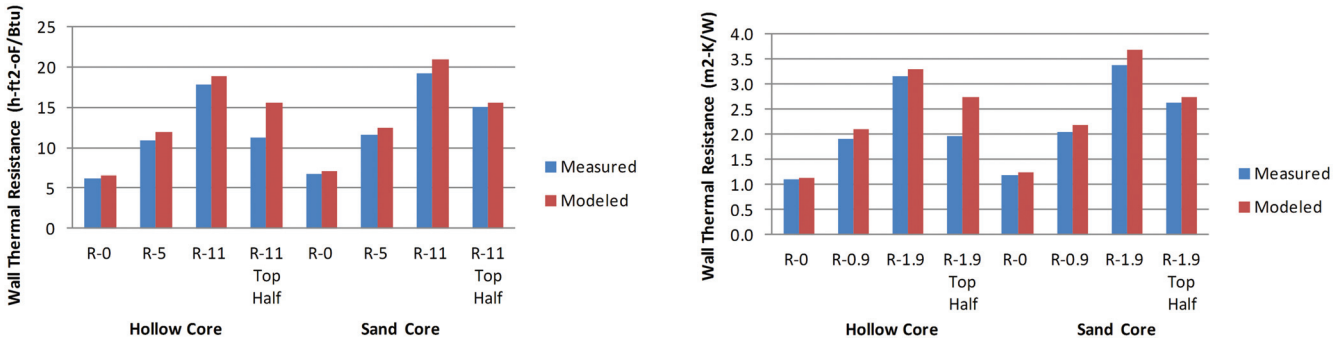

Figure 1 *Measured vs modeled wall R-values: (left) I-P and (right) SI.*

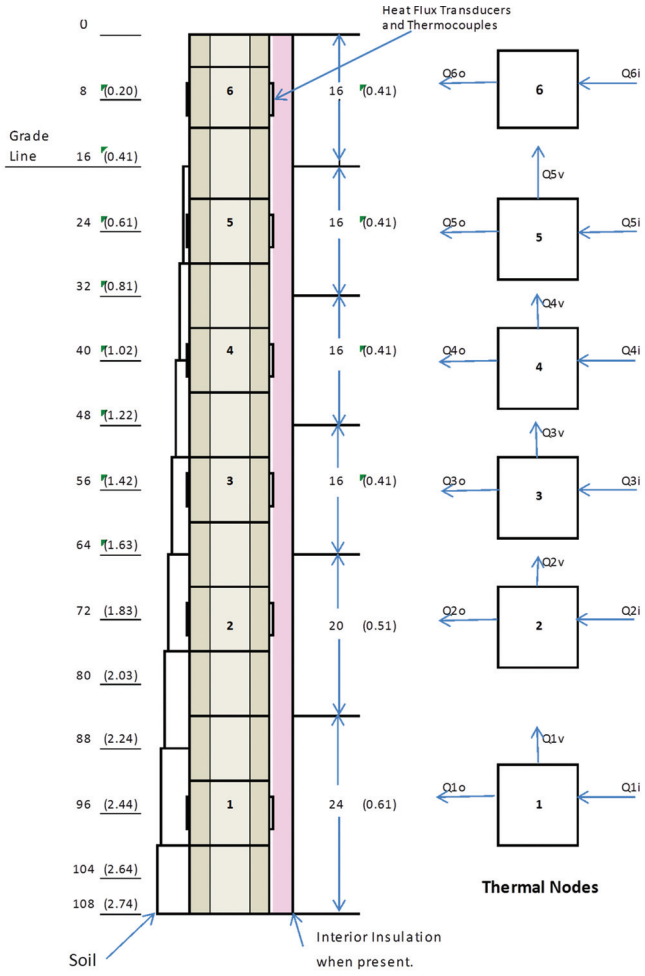

Figure 2 *Wall construction and six thermal nodes, in. (m).*

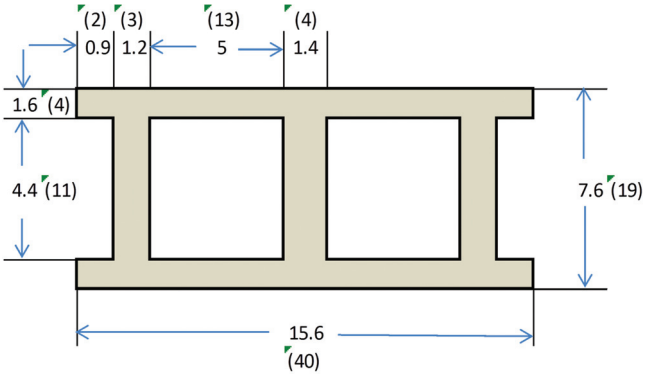

Figure 3 *Masonry block dimensions, in. (cm).*

temperature of 75°F (24°C) and an exterior air temperature of 25°F (–3.9°C).

The masonry block characteristics were: two cores, nominal dimensions of 8 in. (0.20 m) × 8 in. (0.20 m) by 16 in. (0.41 m) (Figure 3), 36 lb (16 kg), and a thermal conductivity of the concrete equal to 0.88 Btu/h·ft·°F (1.5 W/m·K). The thermal conductivity of the sand was 0.13 Btu/h·ft·°F (0.22 W/m·K).

The interior wall insulation configurations were: (1) no insulation, (2) 1 in. (0.03 m) wood furring strips with R-4.8 (R-0.84) insulation plus 0.5 in. (0.01 m) drywall, (3) 24 in. (0.61 m) on center 2 × 4 wood studs, R-11 (R-1.9) insulation full wall plus 0.5 in. (0.03 m) drywall and (4) 24 in. (0.61 m) on center 2 × 4 wood studs full wall, R-11 (R-1.9) insulation on just the top half of the wall plus 0.5 in. (0.01 m) drywall on the entire wall.

The thermal impact of the soil below grade was addressed by installing layers of insulation to the exterior portion of the wall beginning with R-0.8 (R-0.14) for the first foot (0.30 m) below grade and ending with R-15 (R-2.6) at the footer. The thermal conductivity of the soil modeled was 0.78 Btu/h·ft·°F (1.3 W/m·K).

MEASURED RESULTS

The measured results for all eight of the calibrated hot box tests are shown in Tables 1–4. Each table contains the results for the cavity with air and the corresponding results when the cavity was filled with sand. A control volume was defined for each of the thermal nodes and an energy balance was completed which determined the vertical heat flow exiting each node. The vertical heat flow in cavities with air includes natural convection, radiation plus vertical heat transfer through the webs and face shells. The vertical heat flow with sand in cavities includes conduction due to the sand, radiation

but to a much smaller extent and vertical heat transfer through the webs and face shells. The difference between these two vertical heat flows at each node illustrates the vertical heat flow due to natural convection and radiation, see Figures 4–7.

Cavities with sand in the cores reduce the radiation but does not totally eliminate it. The density of sand depends upon the particle size and how tightly the particles are packed. Typical sand densities range from 90 to 112 lb/ft^3 (1442 to 1,794 kg/m^3) while the density of SIO_2 is 165 lb/ft^3 (2,643 kg/m^3)which leads to void volumes of 32 to 45%. Another consideration associated with these particular CHB tests was that the sand was installed in the wall cavities after the wall was built. Sand flowing from the top of the wall to the bottom may not have completely filled in below all of the internal webs leaving voids that would allow some radiation to proceed uninhibited.

ANALYSIS

Natural convection in vertical enclosures can be shown by graphing the Grashof (Gr) number on the horizontal axis and *Ub*/*k* on the vertical axis, see Figure 8.

The solid line (Kreith) shows pure conduction up to Gr = 6×10^3 and then laminar natural convection begins. There is a transition at Gr = 10^5 to fully turbulent flow. Empirical formulas (Jakob) were presented by (Karlekar and Desmond) for 20,000 < Gr < 200,000 as Equation 1.

$$k_e = 0.18k\,\mathrm{Gr}_\delta^{1/4}\,(\delta/L)^{1/9} \qquad (1)$$

where

k_e = effective thermal conductivity, Btu/h·ft·°F (W/m·K)

k = thermal conductivity of air, Btu/h·ft·°F (W/m·K)

Gr = Grashof Number, dimensionless

δ = thickness of the air space, ft (m)

L = height of the air space, ft (m)

For 200,000 < Gr < 10×10^6 use Equation 2.

$$k_e = 0.065k\,\mathrm{Gr}_\delta^{1/3}\,(\delta/L)^{1/9} \qquad (2)$$

Results for these two formulas agree very closely with the solid line. It is important to note that these equations apply to vertical enclosures with interior and exterior surfaces that are of uniform thermal transmittance.

A typical application would be above grade masonry block walls. For example the results of tests conducted in a guarded hot box on masonry block walls are shown in Figure 8 (Van Geem). The Gr number was calculated using the interior and exterior air temperatures as the temperature difference and their average as the mean temperature. These results are consistent with the line for fully turbulent flow (Gr > 1.0×10^5) and Equation 2.

Analysis of the experimental data began by defining six thermal nodes that were aligned with the heat flux transducers and thermocouples installed on the walls, Figure 2. All of the results for each node are presented in Tables 1A–4A in I-P

Table 1A. No Interior Insulation (I-P)

Node	Height in.	Cavity—Hollow					Gr	Cavity—Sand				
		Q_o Btu/h	T_o °F	Q_{vert} Btu/h	Q_i Btu/h	T_i °F		Q_o Btu/h	T_o °F	Q_{vert} Btu/h	Q_i Btu/h	T_i °F
6	16	415.2	45.5	0	274.6	70.8	3.40E+06	368.6	42.2	0	313.3	70.1
5	16	214.7	54.5	140.6	222.4	69.2	1.93E+06	205.1	53.9	55.3	230.2	69.4
4	16	122.5	59.7	132.8	154.0	70.1	1.34E+06	127.0	60.4	30.1	140.9	70.9
3	16	89.1	62.4	101.4	116.0	70.6	1.03E+06	96.7	64.8	16.2	97.6	71.6
2	20	99.5	65.0	74.5	127.3	70.8	7.29E+05	110.6	66.4	15.3	98.0	72.1
1	24	72.8	66.9	46.7	119.5	70.4	4.33E+05	74.9	67.1	27.9	102.8	71.4

Table 2A. R-5 Interior Insulation (I-P)

Node	Height in.	Cavity—Hollow					Gr	Cavity—Sand				
		Q_o Btu/h	T_o °F	Q_{vert} Btu/h	Q_i Btu/h	T_i °F		Q_o Btu/h	T_o °F	Q_{vert} Btu/h	Q_i Btu/h	T_i °F
6	16	226.5	33.3	0	117.0	46.4	2.01E+06	170.8	31.1	0	136.7	42.2
5	16	125.1	40.8	109.4	98.7	48.6	1.15E+06	110.9	38.1	34.0	112.9	45.8
4	16	75.1	44.0	135.8	88.7	50.8	9.81E+05	80.8	45.4	32.1	89.9	51.3
3	16	56.2	46.1	122.2	80.6	52.1	8.53E+05	69.3	50.1	23.0	73.9	54.8
2	20	61.6	49.5	97.8	101.8	53.1	5.08E+05	82.3	54.4	18.3	82.9	58.0
1	24	48.9	51.5	57.6	106.5	54.2	3.69E+05	64	55.8	17.8	81.8	59.3

Table 3A. R-11 Interior Insulation (I-P)

Node	Height in.	Cavity—Hollow					Gr	Cavity—Sand				
		Q_o Btu/h	T_o °F	Q_{vert} Btu/h	Q_i Btu/h	T_i °F		Q_o Btu/h	T_o °F	Q_{vert} Btu/h	Q_i Btu/h	T_i °F
6	16	131	29.5	0	68.4	39.6	1.60E+06	82.3	30.2	0	69.9	36.3
5	16	78.9	34.8	62.5	60.0	41.4	1.01E+06	55.9	42.3	12.4	64.1	39.8
4	16	47.6	38.5	81.2	54.5	43.3	7.30E+05	43.9	42.2	4.2	48.3	45.8
3	16	36.6	40.5	74.3	49.6	44.4	5.86E+05	41.9	48.2	0	41.2	50.7
2	20	39.3	43.4	61.4	64.9	45.7	3.43E+05	50.7	52.3	0.5	47.9	55.0
1	24	30.2	45.4	35.7	65.9	46.9	2.21E+05	37.6	54.9	3.2	40.8	57.0

Table 4A. R-11 Top Half Interior Insulation (I-P)

Node	Height in.	Cavity—Hollow					Gr	Cavity—Sand				
		Q_o Btu/h	T_o °F	Q_{vert} Btu/h	Q_i Btu/h	T_i °F		Q_o Btu/h	T_o °F	Q_{vert} Btu/h	Q_i Btu/h	T_i °F
6	16	189.7	34.5	0	40.4	44.2	1.49E+06	114.8	31.7	0	70.8	39.4
5	16	115.9	41.2	149.2	38.7	48.0	9.99E+05	70.5	41.9	44.0	53.7	41.7
4	16	70.7	45.1	226.3	34.2	50.4	7.68E+05	57	44.9	60.8	31.2	48.4
3	16	58.4	49.3	262.8	165.2	58.4	1.26E+06	62.1	55.2	86.7	126.5	61.7
2	20	66.7	53.2	156.1	144.2	59.0	7.90E+05	75.3	59.5	22.3	72.3	64.4
1	24	50.7	55.0	78.6	129.3	59.1	5.58E+05	51.6	60.5	25.3	76.9	64.1

Table 1B. No Interior Insulation (SI)

Node	Height m	Cavity—Hollow					Gr	Cavity—Sand				
		Q_o W	T_o °C	Q_{vert} W	Q_i W	T_i °C		Q_o W	T_o °C	Q_{vert} W	Q_iQ_i W	T_i °C
6	0.41	121.7	7.5	0.0	80.5	21.6	3.40E+06	108.0	5.7	0.0	91.8	21.2
5	0.41	62.9	12.5	41.2	65.2	20.7	1.93E+06	60.1	12.2	16.2	67.5	20.8
4	0.41	35.9	15.4	38.9	45.1	21.2	1.34E+06	37.2	15.8	8.8	41.3	21.6
3	0.41	26.1	16.9	29.7	34.0	21.4	1.03E+06	28.3	18.2	4.7	28.6	22.0
2	0.51	29.2	18.3	21.8	37.3	21.6	7.29E+05	32.4	19.1	4.5	28.7	22.3
1	0.61	21.3	19.4	13.7	35.0	21.3	4.33E+05	22.0	19.5	8.2	30.1	21.9

Table 2B. R-0.9 Interior Insulation (SI)

Node	Height m	Cavity—Hollow					Gr	Cavity—Sand				
		Q_o W	T_o °C	Q_{vert} W	Q_i W	T_i °C		Q_o W	T_o °C	Q_{vert} W	Q_i W	T_i °C
6	0.41	66.4	0.7	0.0	34.3	8.0	2.01E+06	50.1	–0.5	0.0	40.1	5.7
5	0.41	36.7	4.9	32.1	28.9	9.2	1.15E+06	32.5	3.4	10.0	33.1	7.7
4	0.41	22.0	6.7	39.8	26.0	10.4	9.81E+05	23.7	7.4	9.4	26.3	10.7
3	0.41	16.5	7.8	35.8	23.6	11.2	8.53E+05	20.3	10.1	6.7	21.7	12.7
2	0.51	18.1	9.7	28.7	29.8	11.7	5.08E+05	24.1	12.4	5.4	24.3	14.4
1	0.61	14.3	10.8	16.9	31.2	12.3	3.69E+05	18.8	13.2	5.2	24.0	15.2

Table 3B. R-1.9 Interior Insulation (SI)

Node	Height m	Cavity—Hollow					Gr	Cavity—Sand				
		Q_o W	T_o °C	Q_{vert} W	Q_i W	T_i °C		Q_o W	T_o °C	Q_{vert} W	Q_i W	T_i °C
6	0.41	38.4	–1.4	0.0	20.0	4.2	1.60E+06	24.1	–1.0	0.0	20.5	2.4
5	0.41	23.1	1.6	18.3	17.6	5.2	1.01E+06	16.4	5.7	3.6	18.8	4.3
4	0.41	14.0	3.6	23.8	16.0	6.3	7.30E+05	12.9	5.7	1.2	14.2	7.7
3	0.41	10.7	4.7	21.8	14.5	6.9	5.86E+05	12.3	9.0	0.0	12.1	10.4
2	0.51	11.5	6.3	18.0	19.0	7.6	3.43E+05	14.9	11.3	0.1	14.0	12.8
1	0.61	8.9	7.4	10.5	19.3	8.3	2.21E+05	11.0	12.7	0.9	12.0	13.9

Table 4B. R-1.9 Top Half Interior Insulation (SI)

Node	Height m	Cavity—Hollow					Gr	Cavity—Sand				
		Q_o W	T_o °C	Q_{vert} W	Q_i W	T_i °C		Q_o W	T_o °C	Q_{vert} W	Q_i W	T_i °C
6	0.41	55.6	1.4	0.0	11.8	6.8	1.49E+06	33.6	–0.2	0.0	20.7	4.1
5	0.41	34.0	5.1	43.7	11.3	8.9	9.99E+05	20.7	5.5	12.9	15.7	5.4
4	0.41	20.7	7.3	66.3	10.0	10.2	7.68E+05	16.7	7.2	17.8	9.1	9.1
3	0.41	17.1	9.6	77.0	48.4	14.7	1.26E+06	18.2	12.9	25.4	37.1	16.5
2	0.51	19.5	11.8	45.7	42.3	15.0	7.90E+05	22.1	15.3	6.5	21.2	18.0
1	0.61	14.9	12.8	23.0	37.9	15.1	5.58E+05	15.1	15.8	7.4	22.5	17.8

units and Tables 1B–4B in SI units.The experimental data for each node includes the measured heat flux and temperature at the outside and inside surfaces of the block walls.

A control volume was defined around each thermal node and an energy balance was completed. Beginning with node 1 there was a net vertical heat flow (Q_{vert}). The Grashof number was also calculated for each node and is included in the table. The next step in the analysis was to calculate Ub/k for each node using Equation 3.

$$U = \frac{Q_{vert}}{A(T_i - T_o)} \tag{3}$$

where

Q_{vert} = vertical heat flow, Btu/h (W)

A = area of the thermal node, ft^2 (m^2)

T_i = inside surface temperature of the face shell, °F (°C)

T_o = outside surface temperature of the face shell, °F (°C)

In addition to the following variables:

b = thickness of the cavity, 4.4 in (0.11 m)

k = thermal conductivity of air, Btu/h·ft·°F (W/m·K)

where the thermal conductivity is evaluated at the mean temperature of T_i and T_o.

The analysis for node 2 accounted for the vertical energy flow from node 1 and the net result was an increase in the vertical heat flow from node 2. Analysis of the subsequent nodes exhibited a similar trend through node 4 which had the largest vertical heat flow of any of the nodes for those walls with a constant layer of interior insulation, Figures 4–6. The exception to this was the wall which only had the top half of it insulated, Figure 7 in which node 3 had the largest vertical heat flow. Node 3 was physically located just below the bottom edge of the insulation that had been installed on the top half of the wall. The insulation on the top half of the wall kept the block faces cooler than those on the bottom half of the wall which further enhanced the vertical convection. Proceeding further up the wall the temperature difference between the inside and outside faces of the block begins to decrease which causes the natural convection to decrease.

Figures 4–7 also show the vertical heat flow for the walls which had sand in the cavities. In all cases the vertical heat flow through the walls with cavities that were filled with sand were lower than the vertical heat flow through the walls with cavities that were hollow. Clearly the sand altered the vertical natural convection and radiation heat transfer.

When the results for the four tests for below grade masonry walls with cavities that were hollow are added to Figure 8 substantial departure from the above grade masonry walls was exhibited as expected.

DISCUSSION

The analysis of vertical heat flow due to natural convection in below grade basement walls with cavities that are

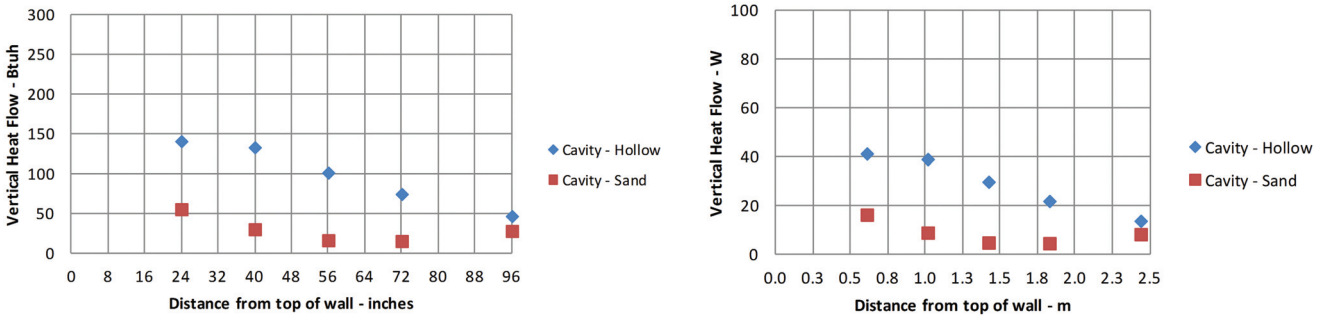

Figure 4 *Vertical heat flow—no interior insulation: (left) I-P and (right) SI.*

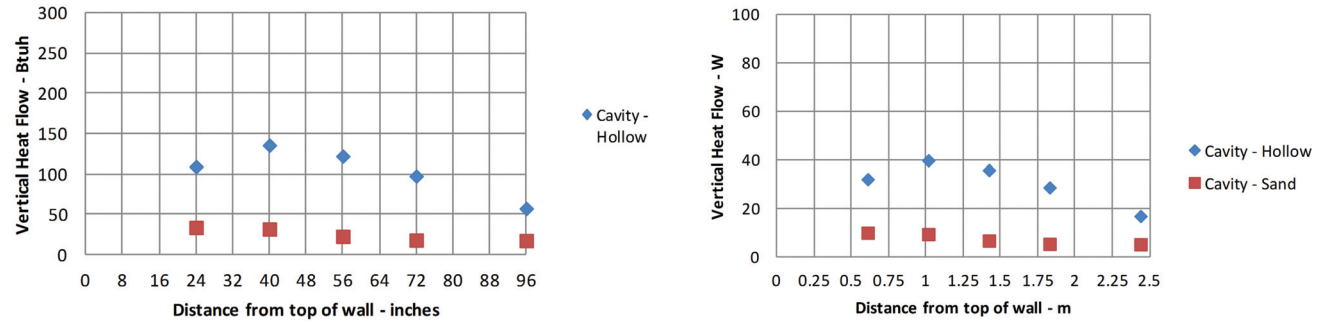

Figure 5 *Vertical heat flow—(left) interior R-5 and (right) interior R-09.*

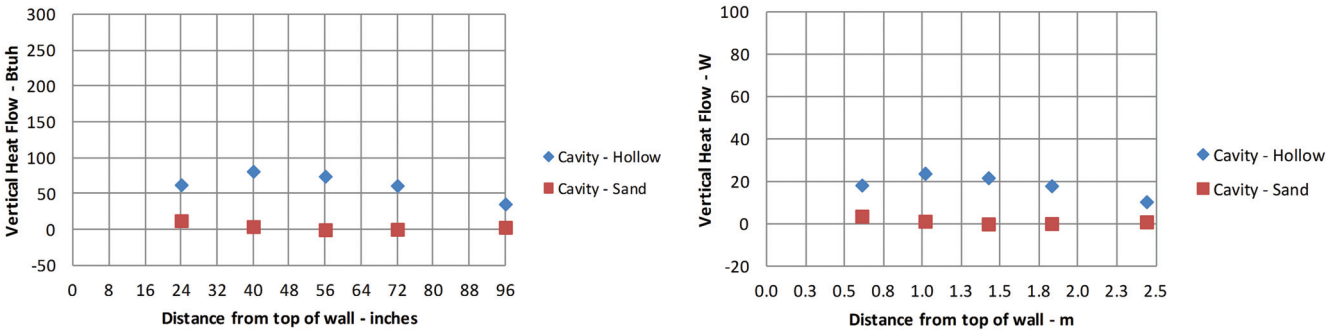

Figure 6 *Vertical heat flow—(left) interior R-11 and (right) interior R-1.9.*

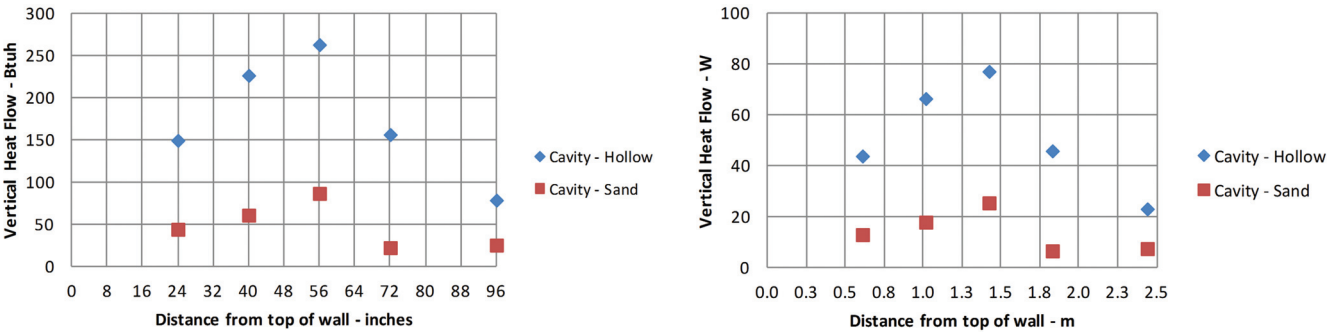

Figure 7 *Vertical heat flow on top—(left) interior R-11 on top half and (right) interior R-1.9.*

hollow has been shown to be very complex. A series of six thermal nodes were analyzed using experimental data for eight test walls. The results exhibited similar trends in that the vertical heat flow due to natural convection increased from the bottom to the top of the walls. The natural convection was shown to be significantly increased due to the impact of the surrounding soil on the exterior. As insulation was added to the interior surface of the wall the natural convection increased

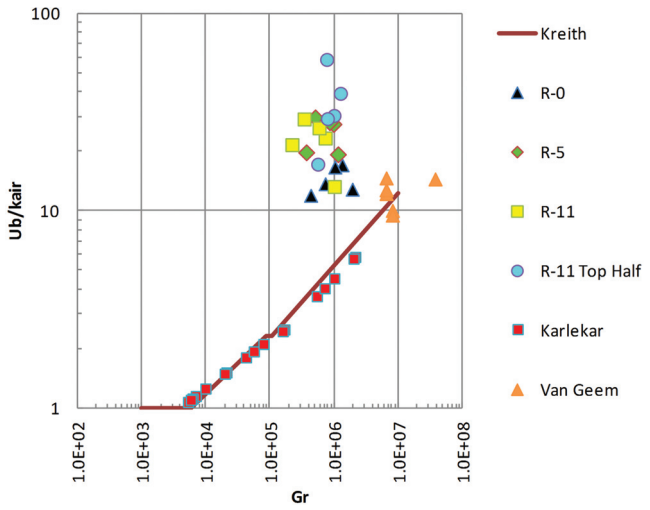

Figure 8 *Vertical air spaces.*

even further. Finally, when only the top half of the interior wall was insulated the natural convection was the highest. For this case only the arc-length method should not be used. Comparisons to prior experimental data quantified the magnitudes of the increased vertical heat flow. The complexity and interactions of the various heat flow mechanisms did not reveal any simplifications that could be made to further improve the arc-length modeling procedures. Any modeling improvements would require a more complex approach which would include a thermal network that coupled all of the nodes identified in this analysis.

CONCLUSION

The primary result of this analysis was the quantification of the vertical heat flow due to natural convection within cavities that were hollow. There was some expectation that the experimental data would exhibit some consistent trends that could be used to develop a simplified model or correlation method that would improve the arc-length calculation procedure for the case with open cavity walls insulated only on the top half. Fundamentally, the scatter is representative of the complex nature of the multiple heat transfer mechanisms that exist with below grade masonry walls. In order to truly model this complexity of vertical heat flow a thermal network would need to be created that coupled the six nodes. Furthermore, there are too few data points in this study to fully develop a predictive model that would be applicable to the broad range of temperature conditions that occur with a typical basement over the course of a year.

NOMENCLATURE

b	=	thickness of an air space, in. (m)
g	=	acceleration due to gravity, ft/sec^2 (m/sec^2)
Gr	=	Grashof Number, dimensionless
k	=	thermal conductivity, Btu/h·ft·°F (W/m·K)
L	=	clearance in enclosed space, ft (m)
Q	=	heat flow, Btu/h (W)
R	=	thermal resistance, h·ft^2·°F/Btu (m^2·K/W)
T	=	temperature, °F (°C)
U	=	thermal transmission, Btu/h·ft^2·°F (W/m·K)

Greek

δ	=	thickness of an air space, ft (m)
β	=	coefficient of volumetric expansion, 1/°F (1/°C)
ρ	=	density of air, lb/ft^3 (kg/m^3)
μ	=	viscosity of fluid, lb/ft·sec (Pa·s)

Subscripts

i	=	inside
e	=	effective
o	=	outside
v	=	vertical

REFERENCES

ASHRAE. 2009. *2009 ASHRAE Handbook—Fundamentals*. Atlanta: American Society of Heating Refrigerating and Air-Conditioning Engineers, Inc.

Jakob, M. 1958. *Heat Transfer*. Wiley, New York, NY.

Karlekar, B.V. and Desmond, R.M. 1977. Engineering Heat Transfer, West Publishing Company, St. Paul. MN.

Kreith, F. 1967. Principles of Heat Transfer, International Textbook Company, Sranton, PA.

McAdams, W.H. 1954. Heat Transmission, McGraw-Hill Book Company, New York, NY.

Shipp, P.H. 1983. Natural Convection within Masonry Block Basement Walls. ASHRAE Transactions, 89 (1B): 405-419.

Van Geem, M.G. 1985. Thermal Transmittance of Concrete Block Walls with Core Insulation. ASHRAE Transactions, 85 (2): 17-35.